

# High-precision half-life determination for the superallowed $\beta^+$ emitter $^{62}\text{Ga}$

G. F. Grinyer,<sup>1,\*</sup> P. Finlay,<sup>1</sup> C. E. Svensson,<sup>1</sup> G. C. Ball,<sup>2</sup> J. R. Leslie,<sup>3</sup> R. A. E. Austin,<sup>4</sup> D. Bandyopadhyay,<sup>1,†</sup> A. Chaffey,<sup>4</sup> R. S. Chakravarthy,<sup>2</sup> P. E. Garrett,<sup>1,2</sup> G. Hackman,<sup>2</sup> B. Hyland,<sup>1</sup> R. Kanungo,<sup>2,‡</sup> K. G. Leach,<sup>1</sup> C. M. Mattoon,<sup>5</sup> A. C. Morton,<sup>2</sup> C. J. Pearson,<sup>2</sup> A. A. Phillips,<sup>1</sup> J. J. Ressler,<sup>6</sup> F. Sarazin,<sup>5</sup> H. Savajols,<sup>2</sup> M. A. Schumaker,<sup>1</sup> and J. Wong<sup>1</sup>

<sup>1</sup>*Department of Physics, University of Guelph, Guelph, Ontario, Canada N1G 2W1*

<sup>2</sup>*TRIUMF, 4004 Wesbrook Mall, Vancouver, British Columbia, Canada V6T 2A3*

<sup>3</sup>*Department of Physics, Queen's University, Kingston, Ontario, Canada K7L 3N6*

<sup>4</sup>*Department of Astronomy and Physics, Saint Mary's University, Halifax, Nova Scotia, Canada B3H 3C3*

<sup>5</sup>*Department of Physics, Colorado School of Mines, Golden, Colorado, 80401 USA*

<sup>6</sup>*Department of Chemistry, Simon Fraser University, Burnaby, British Columbia, Canada V5A 1S6*

(Received 20 August 2007; published 29 January 2008)

The half-life of the superallowed  $\beta^+$  emitter  $^{62}\text{Ga}$  has been measured at TRIUMF's Isotope Separator and Accelerator facility using a fast-tape-transport system and  $4\pi$  continuous-flow gas proportional counter to detect the positrons from the decay of  $^{62}\text{Ga}$  to the daughter  $^{62}\text{Zn}$ . The result,  $T_{1/2} = 116.100 \pm 0.025$  ms, represents the most precise measurement to date (0.022%) for any superallowed  $\beta$ -decay half-life. When combined with six previous measurements of the  $^{62}\text{Ga}$  half-life, a new world average of  $T_{1/2} = 116.121 \pm 0.021$  ms is obtained. This new half-life measurement results in a 20% improvement in the precision of the  $^{62}\text{Ga}$  superallowed  $ft$  value while reducing its mean by  $0.9\sigma$  to  $ft = 3074.3(12)$  s. The impact of this half-life measurement on precision tests of the CVC hypothesis and isospin symmetry breaking corrections for  $A \geq 62$  superallowed decays is discussed.

DOI: [10.1103/PhysRevC.77.015501](https://doi.org/10.1103/PhysRevC.77.015501)

PACS number(s): 21.10.Tg, 23.40.Bw, 24.80.+y, 27.50.+e

## I. INTRODUCTION

Superallowed Fermi  $\beta$  decays between  $0^+$  isobaric analog states have provided an invaluable probe of the Standard Model description of electroweak interactions (see Ref. [1] and references therein). Owing primarily to their relative insensitivity to nuclear structure effects, which enter only as small corrections at the percentage level, these decays have set strict limits on possible extensions to the Standard Model to include scalar and right-handed currents [2], have confirmed the conserved vector current (CVC) hypothesis to 1.3 parts in  $10^4$  [3], and have provided the most precise determination of the CKM matrix element  $V_{ud}$  [3,4]. As a consequence of the CVC hypothesis, which postulates that the vector coupling constant for semileptonic weak interactions  $G_V$  is not renormalized in the nuclear medium, the  $ft$ , and corrected  $ft$  values (denoted  $\mathcal{F}t$ ), for decays between isospin  $T = 1$  isobaric analog states can be expressed as [1]:

$$\mathcal{F}t = ft(1 + \delta'_R)(1 + \delta_{NS} - \delta_C) = \frac{K}{2G_V^2(1 + \Delta_R^V)}, \quad (1)$$

where  $K$  is a constant,  $\Delta_R^V$  is a radiative correction that is nucleus independent, the quantities  $\delta'_R$  and  $\delta_{NS}$  represent corrections for quantum electrodynamics (QED) radiative effects, and  $\delta_C$  is a correction for the breaking of perfect isospin symmetry by Coulomb and charge-dependent nuclear forces. High-precision  $ft$  values have been determined

experimentally to better than 0.1% for nine superallowed transitions between  $14 \leq A \leq 62$ . To maintain this high degree of precision in the corresponding  $\mathcal{F}t$  values the nuclear-structure corrections, which are of the order of 1%, must therefore be understood to within 10% of their value, a demanding requirement of the theoretical calculations.

The calculations of the isospin symmetry breaking corrections  $\delta_C$  are performed using either the model of Towner and Hardy [5], which uses a shell-model diagonalization with a Woods-Saxon plus Coulomb potential, or that of Ormand and Brown [6], which employs a self-consistent Hartree-Fock calculation. These corrections are typically subdivided into two components,  $\delta_C = \delta_{C1} + \delta_{C2}$ , where the first term  $\delta_{C1}$  accounts for different configuration mixing among the  $0^+$  parent and daughter states and the second  $\delta_{C2}$  arises from differences in proton and neutron separation energies that lead to an imperfect overlap of the radial wave functions. There is a small, but systematic, difference between the two models used to calculate  $\delta_C$  that is presently the limiting factor in the overall precision of the world average  $\mathcal{F}t$  value,  $\overline{\mathcal{F}t} = 3073.9 \pm 0.8$  (stat.)  $\pm 0.9(\delta_C)$  s [3], calculated from the 13 superallowed  $\mathcal{F}t$  values that have been determined to better than 0.5%.

High-precision measurements of the  $ft$  values for superallowed transitions in the  $A \geq 62$  region can provide a rigorous test of the theoretical calculations because these decays have larger predicted isospin symmetry breaking corrections ( $> 1\%$ ) and show greater model dependency than in the lighter decays. The superallowed  $ft$  value for  $^{62}\text{Ga}$ , in particular, is presently the most precisely determined in the  $A \geq 62$  region. Its superallowed branching ratio has recently been deduced to high precision, 99.861(11)% [7], using the excited  $2^+$  states in the daughter  $^{62}\text{Zn}$  as collectors for the  $\gamma$ -decay flux from the weak and unobserved  $\beta$ -decay branches to high-lying  $1^+$  states within the  $Q$ -value window. With this result, combined

\*ggrinyer@physics.uoguelph.ca

†Present address: TRIUMF, 4004 Wesbrook Mall, Vancouver, British Columbia, Canada V6T 2A3.

‡Department of Astronomy and Physics, St. Mary's University, Halifax, Nova Scotia, Canada B3H 3C3.

with a recent high-precision  $Q$ -value measurement [8], the  $ft$  value for  $^{62}\text{Ga}$  prior to the present work,  $ft = 3075.6(14)$  s, was limited by the overall precision in the half-life. Although six previous measurements of the  $^{62}\text{Ga}$  half-life have been performed with precisions of  $<0.3\%$ , the previous world average,  $T_{1/2} = 116.17 \pm 0.04$  ms, was dominated by a single measurement,  $T_{1/2} = 116.19 \pm 0.04$  ms [9], that was 4 times more precise than any of the other five measurements. In this work we present the results of a new  $^{62}\text{Ga}$  half-life determination that is 1.6 times more precise and  $2.3\sigma$  lower than that of Ref. [9] and, when combined with all previous half-life measurements, leads to a  $0.9\sigma$  decrease and a 20% improvement in the overall precision of the  $^{62}\text{Ga}$   $ft$  value. This new  $^{62}\text{Ga}$   $ft$  value now rivals the precision of the best measured superallowed decays and leads to an improved test of the theoretical calculations for isospin symmetry breaking corrections in  $A \geq 62$  nuclei.

## II. HALF-LIFE DETERMINATION

### A. Experiment

The  $^{62}\text{Ga}$  half-life experiment was performed at the Isotope Separator and Accelerator (ISAC) facility at TRIUMF in Vancouver, Canada. A radioactive beam of  $\sim 8000$   $^{62}\text{Ga}$  ions/s was produced following the bombardment of a ZrC production target ( $14.78$  g/cm $^2$  Zr) by  $35$   $\mu\text{A}$  of 500-MeV protons from the TRIUMF main cyclotron. Spallation reaction products diffused from the ZrC target surface and were ionized using the TRIUMF Resonant Ionization Laser Ion Source (TRILIS) [10], which was tuned to selectively ionize Ga isotopes. Compared to the  $^{62}\text{Ga}$  beams produced with TRILIS in an earlier experiment [7], the present beam intensity of  $\sim 8000$   $^{62}\text{Ga}$  ions/s in the experiment described here was two times larger, whereas the level of isobaric contamination, specifically  $^{62}\text{Cu}/^{62}\text{Ga} = 0.8(2)$ , was reduced by more than an order of magnitude by using a bare Ta transfer tube without a Re foil to suppress surface ionization. Following laser ionization, mass-separated  $^{62}\text{Ga}$  was extracted as a  $1^+$  ion beam and delivered to a fast-tape-transport system and  $4\pi$  gas proportional counter in the ISAC experimental hall.

The low-energy (30 keV) beam was implanted, under vacuum, into a 25-mm-wide aluminized mylar tape for  $\sim 0.5$  s or approximately 4.5  $^{62}\text{Ga}$  half-lives. Following the collection, the beam was turned off and the sample of  $^{62}\text{Ga}$  was moved rapidly (36 cm in 130 ms) out of vacuum and into a  $4\pi$  proportional counter that has been described previously [11–14]. The gas counter was operated in the plateau region, as determined by a  $^{90}\text{Sr}$  source, which corresponded to voltages between 2600 and 2850 V. The  $\beta$  particles from the decay of the sample were multiscaled using two independent computer automated measurement and control (CAMAC) multichannel scaler modules (MCS's) into 250 bins of adjustable bin-time widths. The bin times were varied on a run-by-run basis between 8, 10, and 12 ms in this experiment. The decay collection time therefore spanned 2.0–3.0 s or 17–26  $^{62}\text{Ga}$  half-lives. Beam pulsing, tape movement intervals, and dwell times were controlled through a Jorway controller in CAMAC. A Stanford Research Systems 1 MHz  $\pm$  1 Hz precision

laboratory clock scaled to 100 kHz was used to provide a time standard for the experiment. The clock was calibrated after the experiment and yielded 99.999397 kHz. Nonextendible and fixed dead times per event of  $\tau_1 \approx 3$   $\mu\text{s}$  and  $\tau_2 \approx 4$   $\mu\text{s}$  were applied to each of the MCS's using two LeCroy 222N nonretriggerable gate-and-delay generators. These dead times were chosen to be much longer than the series dead times in the system and were measured to be  $\tau_1 = 2.9489 \pm 0.0079$   $\mu\text{s}$  and  $\tau_2 = 3.9671 \pm 0.0079$   $\mu\text{s}$  using the source-plus-pulsar technique [15]. One dead time was applied to each of the MCS's and they were interchanged throughout the experiment to investigate possible systematic effects. To further explore potential systematics associated with the electronics, the detector operating voltage, lower-level-discriminator threshold, and dwell times were also altered on a run-by-run basis.

### B. Data preselection

A total of 83445 cycles were collected in this experiment. In the offline analysis, a threshold (unique to each run) was set that rejected any cycles for which the total number of counts fell below a prescribed value. This rejection criterion removed a total of 6417 cycles and were all those cycles in which the primary proton beam had tripped off. A second criterion used the ratio of the number of counts recorded by the  $4\pi$  gas counter to that of a scintillator located at the beam implantation site to reject 3242 cycles where the  $^{62}\text{Ga}$  sample was not accurately centered within the gas counter. The 9659 cycles (11.6% of the total number of cycles collected) rejected by these criteria were among the poorest statistically and contained only 5.9% of the raw data.

### C. Results

Following the preselection criteria described above, a total of 73786 cycles remained, divided among 56 experimental runs of approximately equal duration. Each cycle was dead-time corrected using the procedure of Refs. [13,14] and the measured dead times (see Sec. II A). The maximum detector rate was  $\sim 4000$  counts/s, which corresponded to a maximum dead-time correction of  $\sim 3\%$  at  $t = 0$ . The dead-time-corrected decay data were fit using a  $\chi^2$  minimization routine [16] that employs the  $\chi^2$  derived from a direct application of maximum likelihood to the Poisson probability distribution. This procedure has been shown to introduce negligible bias in counting experiments with small numbers of counts per bin [17] and has been universally adopted in the evaluation of superallowed  $\beta$ -decay data [1].

To test for the presence of isobaric contaminants in the mass-separated  $A = 62$  beam, a  $\beta$ - $\gamma$  coincidence spectrum was obtained [18] using the 20 HPGe detectors of the  $8\pi$   $\gamma$ -ray spectrometer [19] and the 20 plastic scintillators of the scintillating electron-positron tagging array (SCEPTAR) [20,21]. The beam-on time was 30 s (as opposed to 0.5 s in the half-life measurement) in order to enhance the relative activities of the longer-lived isobars. From the  $\beta$ - $\gamma$  coincidence spectrum shown in Fig. 1, isobaric contamination from  $^{62}\text{Cu}$  ( $T_{1/2} = 9.67(3)$  min [22,23]),  $^{62}\text{gCo}$  ( $T_{1/2} = 1.50(4)$  min [23]), and  $^{62\text{m}}\text{Co}$  ( $T_{1/2} = 13.91(5)$  min [23]) was observed. Relative

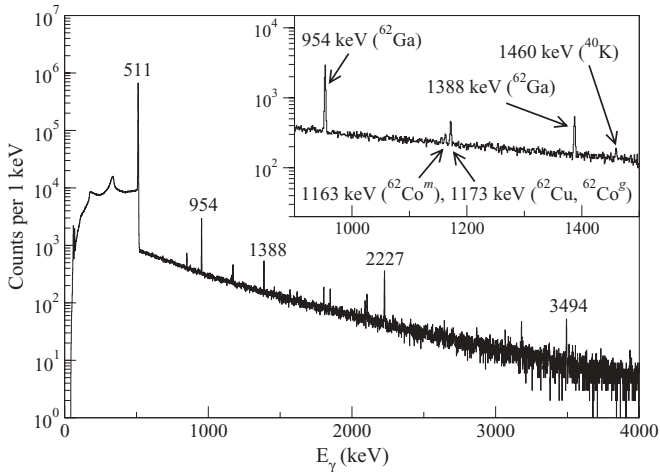


FIG. 1. Summed  $\gamma$ -ray spectrum from the 20 HPGe detectors of the  $8\pi$  spectrometer when detected in coincidence with a  $\beta$  particle in the SCEPTAR array. (Inset) Isobaric contamination from the decays of  $^{62}\text{Cu}$ ,  $^{62g}\text{Co}$ , and  $^{62m}\text{Co}$  was directly observed while upper limits were deduced on the possible contributions from  $^{62}\text{Mn}$  and  $^{62}\text{Fe}$ .

yields of these isobars, with respect to  $^{62}\text{Ga}$ , were calculated with the known  $\beta$ -branching ratios [23] and a relative HPGe efficiency calibration using standard  $^{56}\text{Co}$ ,  $^{133}\text{Ba}$ , and  $^{152}\text{Eu}$  sources [18]. These relative yields were subsequently converted into relative activities at  $t = 0$  in the gas counter using the beam-on (grow-in) time of 0.5 s and the tape transit time to the gas counter of 0.13 s. The relative yields,  $R_{\text{rel}}$ , and activities (at  $t = 0$ ),  $A_{\text{rel}}$ , in the half-life experiment are summarized in Table I. Although the  $\gamma$ -ray photopeaks expected from the decays of  $^{62}\text{Mn}$  ( $T_{1/2} = 0.88(15)$  s [23,24]) and  $^{62}\text{Fe}$  ( $T_{1/2} = 68(2)$  s [23]) were not observed, upper limits were set on their existence using the  $+1\sigma$  uncertainties following null-area fits to the expected locations of the photopeaks. The  $8\pi$  spectrometer and the  $4\pi$   $\beta$  counting station utilize the same central beam line at ISAC that leads from the target and ion source through the mass separator and into the experimental hall. Once inside the experimental facility, beams are delivered to both of these stations via separate beam lines stemming from the central delivery line. Because the target, ion source, and mass separator are common to both experiments, isobaric beam contamination is therefore considered to be the same at both

TABLE I. Isobaric contamination in the  $A = 62$  beam deduced from  $\beta$ - $\gamma$  coincidences between the 20 HPGe detectors of the  $8\pi$  spectrometer and the 20 plastic scintillators of the SCEPTAR array. The relative yields  $R_{\text{rel}}$  and activities  $A_{\text{rel}}$  in the half-life measurement at  $t = 0$  are calculated (following a 0.5 s grow-in time and 0.13 s tape movement) relative to  $^{62}\text{Ga}$ .

Decay parent	$T_{1/2}$	$R_{\text{rel}}$	$A_{\text{rel}}$
$^{62}\text{Ga}$	116.17(4) ms	1.0	1.0
$^{62}\text{Cu}$	9.67(3) min	0.79(19)	$1.12(27) \times 10^{-3}$
$^{62g}\text{Co}$	1.50(4) min	$3.0(14) \times 10^{-4}$	$2.8(13) \times 10^{-6}$
$^{62m}\text{Co}$	13.91(5) min	$3.5(6) \times 10^{-3}$	$3.5(6) \times 10^{-6}$
$^{62}\text{Fe}$	68(2) s	$<4.3 \times 10^{-3}$	$<5.3 \times 10^{-5}$
$^{62}\text{Mn}$	0.88(15) s	$<4.7 \times 10^{-6}$	$<3.3 \times 10^{-6}$

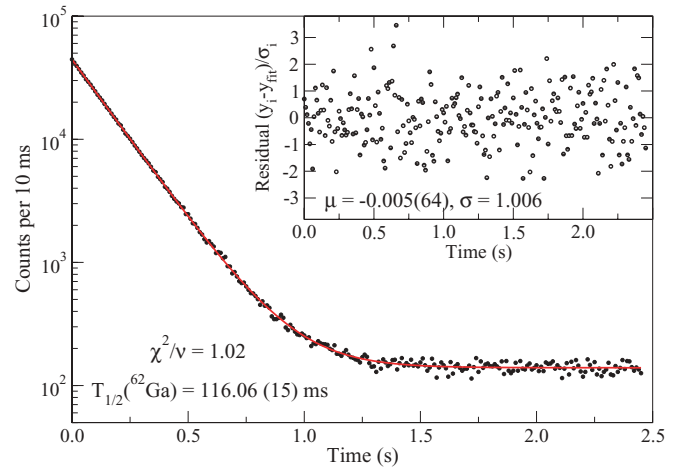


FIG. 2. (Color online) Typical dead-time-corrected decay curve from a single  $^{62}\text{Ga}$  run (run 23) summed over 1668 cycles. (Inset) The residuals;  $(y_i - y_{\text{fit}})/\sigma_i$ , although not used directly in the Poisson maximum likelihood fit, remain a measure of the goodness of fit and yield a mean of  $\mu = -0.005(64)$  and standard deviation of  $\sigma = 1.006$ , values that are consistent with the expectation of a normal distribution.

experimental stations. In addition, the  $8\pi$  yield experiment was performed immediately after the half-life experiment, and the measured contaminant ratios are expected to differ by much less than 20% (the most precisely determined ratio in Table I) in these subsequent measurements.

The cycle-by-cycle dead-time-corrected decay data were summed into a single decay curve for each experimental run, corrected by the clock calibration (see Sec. II A), and were fit to a function that contained four exponentials ( $^{62}\text{Ga}$ ,  $^{62}\text{Cu}$ ,  $^{62g}\text{Co}$ ,  $^{62m}\text{Co}$ ) plus a constant background. The  $t = 0$  relative activities and half-lives for each of the contaminants were fixed at the central values listed in Table I. The fit function therefore contained only three free parameters: (i) the activity of  $^{62}\text{Ga}$  at  $t = 0$ , (ii) the half-life of  $^{62}\text{Ga}$ , and (iii) the constant background rate. This procedure is defined as the “best-fit” result for extracting the half-life of  $^{62}\text{Ga}$ . In Sec. II D below, the effects of the uncertainties on these fixed parameters are considered and are tested for consistency in the fitting procedure by using additional permutations of the fit function, including the upper limits of  $^{62}\text{Mn}$  and  $^{62}\text{Fe}$  isobaric contamination. A sample dead-time-corrected decay curve, resulting fit, and corresponding residuals;  $(y_i - y_{\text{fit}})/\sigma_i$ , from a single run (Run 23, 1668 cycles) is presented in Fig. 2.

The half-lives of  $^{62}\text{Ga}$  obtained from each of the 56 runs (with statistical uncertainties) are shown in Fig. 3. A weighted average of these 56 runs yields the  $^{62}\text{Ga}$  half-life (and statistical uncertainty) deduced in this work,  $T_{1/2} = 116.100 \pm 0.022$  ms, with a reduced  $\chi^2$  value of 0.77.

#### D. Systematic uncertainties

Two separate and independent multichannel scalers were used to bin the decay data, with each MCS receiving a different fixed and nonextendible dead time of either 3 or 4  $\mu\text{s}$ . These dead times were periodically swapped throughout the

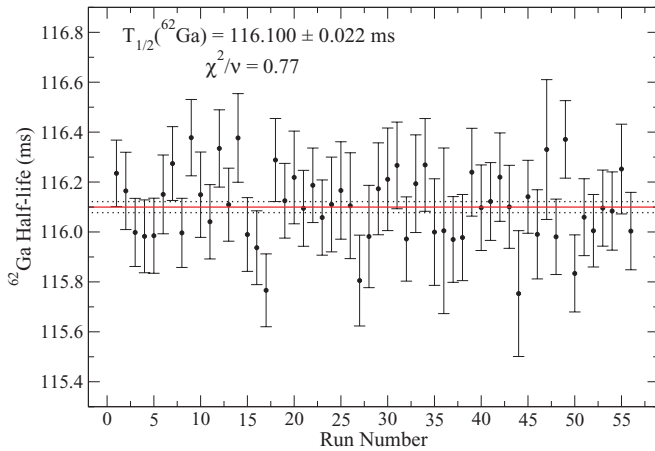


FIG. 3. (Color online) Half-life of  $^{62}\text{Ga}$  (with statistical uncertainties) versus the experimental run number. The weighted average of all 56 runs and its statistical uncertainty  $T_{1/2} = 116.100 \pm 0.022$  ms are displayed as horizontal solid and dotted lines, respectively.

experiment. The half-lives of  $^{62}\text{Ga}$  obtained using each of the MCS data streams were  $T_{1/2}^{\text{MCS1}} = 116.101 \pm 0.022$  ms and  $T_{1/2}^{\text{MCS2}} = 116.099 \pm 0.022$  ms. Because the two scalers independently bin the same decay data, these are not independent measurements of the  $^{62}\text{Ga}$  half-life but instead provide an important consistency check of the dead-time corrections. Because these two values are consistent, the unweighted average,  $T_{1/2} = 116.100 \pm 0.022$  ms, is adopted as the half-life of  $^{62}\text{Ga}$ . The data shown in Fig. 3 already includes this unweighted average, for each run, of the two MCS data streams. As demonstrated in Fig. 4, separation of the data set into the two dead-time values of 3 and 4  $\mu\text{s}$  yielded identical results of  $T_{1/2} = 116.100 \pm 0.022$  ms for the  $^{62}\text{Ga}$  half-life.

To test for further potential systematic uncertainties, several electronic settings were modified throughout the experiment

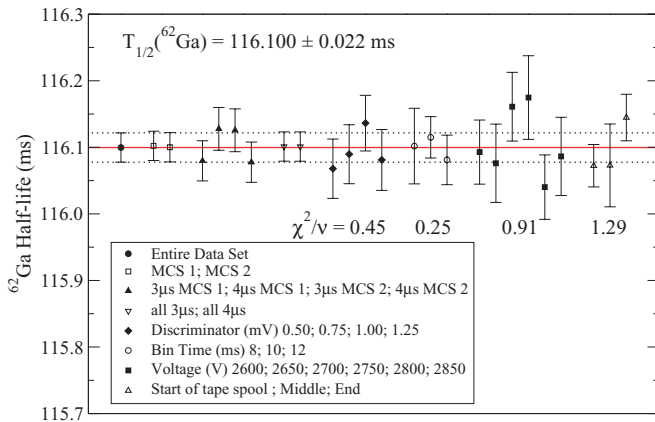


FIG. 4. (Color online) Half-life measurements of  $^{62}\text{Ga}$  (with statistical uncertainties) sorted by adjustable electronic and experimental settings. All reduced  $\chi^2$  values for the independent groups are less than unity with the exception of the tape position value  $\chi^2/\nu = 1.29$ , which is used to estimate possible sources of systematic uncertainty in this analysis.

on a run-by-run basis. These modifications included altering the detector voltage within the plateau region (2600–2850 V), changing the MCS bin times (and hence the decay time length) between 8 ms/bin (2.0 s decay) and 12 ms/bin (3.0 s decay), and adjusting the lower-level-discriminator threshold between 50 and 125 mV. A summary of the  $^{62}\text{Ga}$  half-life obtained at each of the adjustable settings considered is shown in Fig. 4. Of the 56 runs collected in this experiment 15 were obtained using a lower-level-discriminator setting of 50 mV, 14 were at 75 mV, 14 at 100 mV, and 13 at 125 mV. Because this group of four settings contain all of the experimental data, the weighted average of these four groups is the total average,  $T_{1/2} = 116.100 \pm 0.022$  ms. Treating these four settings as four independent measurements of the  $^{62}\text{Ga}$  half-life (with three degrees of freedom) a reduced  $\chi^2$  value of 0.45 is obtained. According to the method of the Particle Data Group [25] a reduced  $\chi^2$  value that is less than unity indicates that the  $^{62}\text{Ga}$  half-life obtained is consistent with there being no systematic uncertainty associated with the four discriminator settings. A similar analysis was performed using the three bin-time values of 8, 10, and 12 ms (2 DOF,  $\chi^2/\nu = 0.25$ ) and the six gas-counter voltage settings of 2600, 2650, 2700, 2750, 2800, and 2850 V (5 DOF,  $\chi^2/\nu = 0.91$ ), indicating that these groups are also consistent with there being no systematic uncertainties pertaining to these settings.

Although not an electronic setting, a fourth grouping was considered that combined the data according to the beam implantation position within the tape spool. The aluminized mylar tape at the  $\beta$  counting station is not a continuous loop but is collected on a spool. Due to its finite length, it was necessary to rewind the tape after every second or third run, which permitted a grouping of the data based on whether the run was obtained before or immediately after a tape rewind. Of the 56 runs collected in this experiment, 25 were obtained after a rewind (at the beginning of the tape spool), 25 were obtained before a rewind (at the end of the tape spool), and 6 were obtained in the middle of the tape when three experimental runs were collected between tape rewinds. The reduced  $\chi^2$  value obtained from these three settings (with two degrees of freedom) is  $\chi^2/\nu = 1.29$ . Although we are unaware of any potential systematic effect associated with the tape spool location we adopt the method of the Particle Data Group [25] and inflate our statistical uncertainty of 0.022 ms by the square root of the reduced  $\chi^2$  value, which leads to an overall uncertainty of 0.025 ms. Assuming the statistical and systematic uncertainties are independent quantities and can be combined in quadrature to obtain the overall uncertainty, the half-life of  $^{62}\text{Ga}$  deduced in this work is  $T_{1/2} = 116.100 \pm 0.022(\text{stat.}) \pm 0.012(\text{sys.})$  ms.

To test for any residual rate dependence in our result, leading channels were removed from the data set in increments of two channels ( $\sim 20$  ms) to a maximum of 36 channels or  $\sim 3$   $^{62}\text{Ga}$  half-lives. The result of this analysis is presented in Fig. 5 and demonstrates that the half-life of  $^{62}\text{Ga}$  deduced in this work is consistent even when three half-lives, or 88% of the data, has been removed from the analysis. Because the beam intensity from TRILIS fluctuated between 4000 to 8000  $^{62}\text{Ga}$  ions/s, a complementary test for residual rate dependencies was performed by plotting the cycle-averaged detector rate at

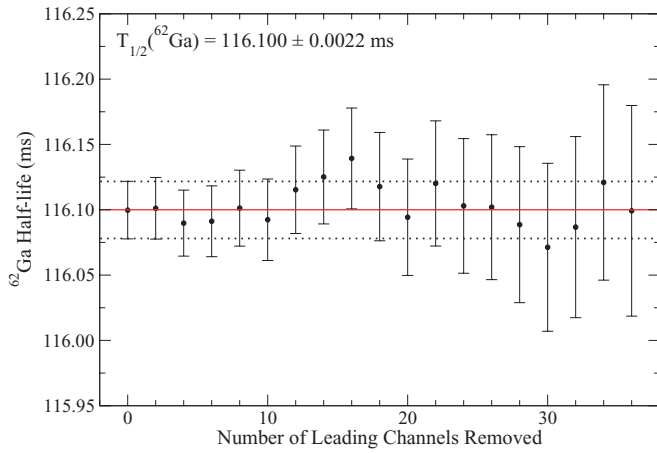


FIG. 5. (Color online) Deduced half-life of  $^{62}\text{Ga}$  (with statistical uncertainties) as a function of the number of leading channels removed from the analysis with the half-life and statistical uncertainty (at 0 channels removed) overlaid for comparison. The  $^{62}\text{Ga}$  half-life obtained in this work remains constant even after three half-lives, or 88% of the data set, have been removed. These data are not randomly scattered about the mean because they are highly correlated with each data point containing all of the data to the right of it.

the start of the decay curve versus the half-life obtained for each of the 56 runs. A weighted linear regression applied to these data resulted in a slope of  $(-1.7 \pm 3.0) \times 10^{-8} \text{ s}^2$  and therefore confirms the expectation that the deduced half-life is rate independent.

Tests of the fit function were investigated by refitting the decay-curve data to a variety of functions that either included or removed the contributions of the various isobaric contaminants. The largest contamination in this experiment came from the decay of  $^{62}\text{Cu}$ , which had a relative activity at  $t = 0$  of only  $1.12(27) \times 10^{-3}$  (see Table I) and a half-life ( $\sim 10$  min) that was very long on the data collection time scale of 2.0–3.0 s used in this experiment. The data were refit using only a single exponential ( $^{62}\text{Ga}$  decay) plus a free constant background under the assumption that the  $^{62}\text{Cu}$  activity could be approximated by a flat background. The result of this analysis yielded  $T_{1/2} = 116.101 \pm 0.022$  ms and is in excellent agreement with the best-fit result that used four exponential decays plus a constant background. This analysis demonstrates the independence of the final result on the low levels of isobaric contamination and any small variation in this ratio between the half-life measurement and the  $\gamma$ -ray experiment with the  $8\pi$  spectrometer that was used to fix the relative contaminant activities. The data were also refit under the assumption that all of the background was due to the decay of  $^{62}\text{Cu}$  and obtained  $T_{1/2} = 116.097 \pm 0.022$  ms for the  $^{62}\text{Ga}$  half-life, which is again in excellent agreement with the best-fit result.

To test for additional sources of systematic uncertainty associated with possible isobaric contamination from  $^{62}\text{Mn}$  and  $^{62}\text{Fe}$  decay, these exponential decays were added to the fit function with their half-lives and intensities fixed at the values listed in Table I. The fit function in each case consisted of five exponential decays plus a constant background (three free parameters) and yielded  $T_{1/2} = 116.098 \pm 0.022$  ms for

TABLE II. Differences  $|\Delta_T|$  between the best-fit  $^{62}\text{Ga}$  half-life using parameters fixed at their central values and the result obtained when these parameters were fixed at their  $\pm 1\sigma$  uncertainties. Treating each of these parameters independently, a total estimate of the systematic uncertainty is obtained from the quadrature sum.

Fixed parameter	Value	$ \Delta_T $ (ms)
Intensity $I(^{62}\text{Cu}/^{62}\text{Ga})$	$1.12(27) \times 10^{-3}$	$\pm 5.8 \times 10^{-4}$
Half-life $T_{1/2}(^{62}\text{Cu})$	9.67(3) min	$\pm 6.7 \times 10^{-6}$
Intensity $I(^{62g}\text{Co}/^{62}\text{Ga})$	$2.8(13) \times 10^{-6}$	$\pm 1.8 \times 10^{-5}$
Half-life $T_{1/2}(^{62g}\text{Co})$	1.50(4) min	$\pm 1.0 \times 10^{-6}$
Intensity $I(^{62m}\text{Co}/^{62}\text{Ga})$	$3.5(6) \times 10^{-6}$	$\pm 9.7 \times 10^{-7}$
Half-life $T_{1/2}(^{62m}\text{Co})$	13.91(5) min	$\pm 2.6 \times 10^{-8}$
Include $I(^{62}\text{Mn}/^{62}\text{Ga})$	$3.3 \times 10^{-6}$	$\pm 1.7 \times 10^{-3}$
Half-life $T_{1/2}(^{62}\text{Mn})$	0.88(15) s	$\pm 3.6 \times 10^{-4}$
Alternate $T_{1/2}(^{62}\text{Mn})$	0.67(5) s	$\pm 1.4 \times 10^{-4}$
Include $I(^{62}\text{Fe}/^{62}\text{Ga})$	$5.3 \times 10^{-5}$	$\pm 9.7 \times 10^{-4}$
Half-life $T_{1/2}(^{62}\text{Fe})$	68(2) s	$\pm 9.4 \times 10^{-4}$
Measured dead times	2.9489(79) $\mu\text{s}$	$\pm 7.7 \times 10^{-4}$
	3.9671(79) $\mu\text{s}$	
Total		0.0024 ms

the half-life of  $^{62}\text{Ga}$  when the  $^{62}\text{Mn}$  upper limit was included and  $T_{1/2} = 116.099 \pm 0.022$  ms when including only  $^{62}\text{Fe}$ . Because  $^{62}\text{Mn}$  and  $^{62}\text{Fe}$  decay were not directly observed in the  $\beta$ - $\gamma$  coincidence spectrum we do not adjust the best-fit value for the half-life of  $^{62}\text{Ga}$  but rather use the differences between these values and the best-fit answer ( $\Delta_T = 1.7 \times 10^{-3}$  ms for  $^{62}\text{Mn}$ ) as a measurement of unaccounted for systematic uncertainties in the best-fit result. A recent measurement of the  $^{62}\text{Mn}$  half-life  $T_{1/2} = 0.67(5)$  s [26] is significantly lower than the value  $T_{1/2} = 0.88(15)$  s [23,24]. If the most recent value is used in this analysis, the  $^{62}\text{Ga}$  half-life deduced is  $T_{1/2} = 116.098 \pm 0.022$  ms, and differs from the value above by only  $\Delta_T = 1.4 \times 10^{-4}$  ms. This difference, which arises from a systematic uncertainty in the  $^{62}\text{Mn}$  half-life, is also included in the total estimate of the systematic uncertainty in this work.

A similar procedure was adopted to account for additional sources of systematic uncertainty associated with fixing specific parameters in the analysis at their central values. For all of the parameters that were fixed to arrive at the best-fit answer the above analysis was repeated for each parameter fixed at  $\pm 1\sigma$  from its central value. The differences between the best-fit result of  $T_{1/2} = 116.100 \pm 0.022$  ms and the half-life obtained using the  $\pm 1\sigma$  values are summarized in Table II for all fixed parameters. A total systematic uncertainty associated with fixing parameters is 0.0024 ms and is obtained from the quadrature sum of the  $\Delta_T$  column in Table II. This uncertainty is negligible when combined in quadrature with the statistical uncertainty of 0.022 ms. The half-life of  $^{62}\text{Ga}$  deduced in this work is therefore  $T_{1/2} = 116.100 \pm 0.022(\text{stat.}) \pm 0.012(\text{sys.})$  ms.

### E. Comparison to previous results

The half-life of  $^{62}\text{Ga}$  deduced in this work (adding the statistical and systematic uncertainties in quadrature) is  $T_{1/2} = 116.100 \pm 0.025$  ms and represents the most precise

TABLE III. Summary of all high-precision  $^{62}\text{Ga}$  half-life measurements. The new world average of  $T_{1/2} = 116.121 \pm 0.0021$  s with a reduced  $\chi^2$  value of 1.006 is obtained from a weighted average of these seven measurements.

Reference	Year	$T_{1/2}$ (ms)	$\sigma$ (ms)
Present work	2007	116.100	0.025
B. Hyland <i>et al.</i> [31]	2005	116.01	0.19
G. Canchel <i>et al.</i> [30]	2005	116.09	0.17
B. Blank <i>et al.</i> [9]	2004	116.19	0.04
B. C. Hyman <i>et al.</i> [29]	2003	115.84	0.25
C. N. Davids <i>et al.</i> [28]	1979	116.34	0.35
D. E. Alburger [27]	1978	115.95	0.30
World average ( $\chi^2/\nu = 1.006$ )		116.121	0.021

measurement of any superallowed half-life to date. Compared to previous measurements of the  $^{62}\text{Ga}$  half-life (Table III, Fig. 6), the result presented here is a factor of 1.6 times more precise than that in Ref. [9] and is 7 times more precise than any of the other five previous determinations [27–31]. A weighted average of all seven half-life measurements shown in Fig. 6 and Table III yields the world average  $T_{1/2} = 116.121 \pm 0.021$  ms. This value is 0.04% or  $2.3\sigma$  lower than the previous world average [1] and reflects the fact that the value deduced by Ref. [9] does not agree with our measurement at the level of 0.08% or  $2.3\sigma$ . Although the reason for the discrepancy between the two highest precision measurements is not understood, the reduced  $\chi^2$  value obtained from the full set of seven  $^{62}\text{Ga}$  half-life measurements is 1.006. Treated as a group, the seven measurements of the  $^{62}\text{Ga}$  half-life is therefore a consistent set and the uncertainty on the world average need not be increased according to the method of the Particle Data Group. As a result of the high-precision half-life determination presented in this work, the average  $^{62}\text{Ga}$  half-life has thus been decreased by  $2.3\sigma$  to  $T_{1/2} = 116.121 \pm 0.021$  ms and its

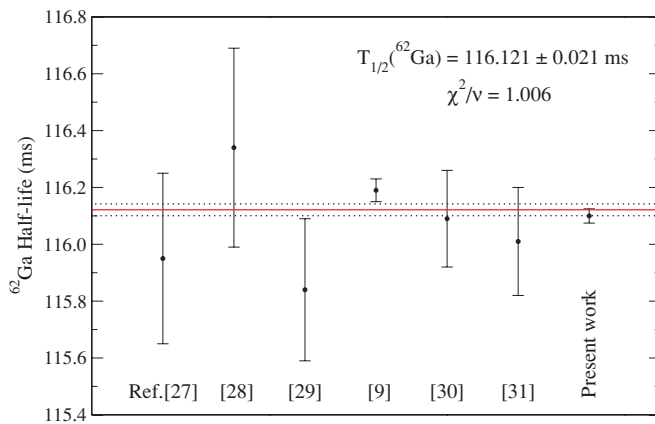


FIG. 6. (Color online) Comparison of all high-precision  $^{62}\text{Ga}$  half-life measurements. The new world average of  $T_{1/2} = 116.121 \pm 0.0021$  ms with a reduced  $\chi^2$  value of 1.006 is obtained from a weighted average of these seven measurements and is overlaid for comparison.

overall precision of 0.018% has been improved upon by nearly a factor of 2. The half-life of  $^{62}\text{Ga}$  is now the most precisely determined superallowed half-life.

### III. ISOSPIN SYMMETRY BREAKING AND THE $^{62}\text{Ga}$ $ft$ AND $\mathcal{F}t$ VALUES

With the significant decrease of  $2.3\sigma$  (0.04%) to the average  $^{62}\text{Ga}$  half-life, the experimental  $ft$  value for this decay, which was previously known to 0.05% and was limited by the uncertainty in the half-life, is also significantly affected. Combining the world-averaged  $^{62}\text{Ga}$  half-life,  $T_{1/2} = 116.121(21)$  ms, with the superallowed branching ratio  $\text{BR} = 99.861(11)\%$  [7], the calculated electron conversion fraction  $P_{\text{EC}} = 0.137\%$  [1], and the statistical rate function  $f = 26401.6(83)$  [8], the result  $ft = 3074.3(3)_{\text{BR}}(5)_{T_{1/2}}(10)_f$  s = 3074.3(12) s is obtained. This result is precise to 0.04% and is now limited by the precision in the  $Q$  value. As a result of the half-life measurement presented in this work, the  $^{62}\text{Ga}$   $ft$  value has been decreased by  $0.9\sigma$  and its overall precision has been improved by more than 20% compared with its previous value [7]. With this 20% improvement, the  $^{62}\text{Ga}$   $ft$  value is now one of the most precisely determined for any of the superallowed decays.

Using the correction terms of  $\delta'_R = 1.459(87)\%$  [32],  $\delta_{\text{NS}} = -0.036(20)\%$  [32], and  $\delta_C = 1.38(16)\%$  [5] the corrected  $ft$  value obtained for  $^{62}\text{Ga}$  is  $\mathcal{F}t = 3074.9(6)_{\delta_{\text{NS}}}(12)_{ft}(26)_{\delta'_R}(50)_{\delta_C}$  s = 3074.9(58) s, a result that has been reduced by 0.9 s compared to its previous value [7] due to the half-life measurement presented here. This result is in excellent agreement with the world average  $\overline{\mathcal{F}t} = 3073.9(8)$  s [3], as expected by the CVC hypothesis, but is entirely limited in precision by the theoretical corrections for isospin symmetry breaking  $\delta_C$  and radiative effects  $\delta'_R$ . A test of the  $\delta_C$  corrections can be performed by calculating the isospin symmetry breaking correction that is required to satisfy the CVC hypothesis. Using the value of  $\overline{\mathcal{F}t} = 3073.9(8)$  s [3], the value  $\delta_C = 1.41(2)_{\delta_{\text{NS}}}(3)_{\overline{\mathcal{F}t}}(4)_{ft}(9)_{\delta'_R}\%$  = 1.41(10)% is obtained for the isospin symmetry breaking correction for  $^{62}\text{Ga}$ . This result is in excellent agreement with the Woods-Saxon model calculations of Towner and Hardy that predict  $\delta_C = 1.38(16)\%$  [5]. A similar test of the self-consistent Hartree-Fock calculations was performed using the world-average  $\mathcal{F}t$  value  $\overline{\mathcal{F}t} = 3075.7(8)$  s obtained with the  $\delta_C$  corrections of Ormand and Brown [6]. The result,  $\delta_C = 1.36(10)\%$ , also agrees with the calculated range of values  $\delta_C = 1.26\text{--}1.32\%$  [6].

The value for  $\delta_C$ , deduced under the assumption that CVC is satisfied, is 1.6 times more precise than the theoretical values and may be used to further constrain the theoretical calculations of isospin symmetry breaking in  $A \geq 62$  superallowed  $\beta$  decays. We note, however, that the deduced value of  $\delta_C$  for  $^{62}\text{Ga}$  is now entirely limited by the uncertainty in the  $\delta'_R$  calculation for this high- $Z$  superallowed emitter. A significant sharpening of this test of the isospin symmetry breaking corrections could thus be achieved with a reduction in the uncertainties of  $\delta'_R$  for the heavy superallowed emitters by extending the radiative corrections to higher order [33].

#### IV. CONCLUSION

The half-life of the superallowed  $\beta^+$  emitter  $^{62}\text{Ga}$  has been deduced using a  $4\pi$  proportional counter and fast-tape-transport system at TRIUMF's ISAC facility. The result,  $T_{1/2} = 116.100 \pm 0.025$  ms, is the most precise measurement of any superallowed half-life to date and leads to a  $2.3\sigma$  decrease in the  $^{62}\text{Ga}$  world-average half-life. The new world average, obtained from a weighted average of all seven measurements to date, yields  $T_{1/2} = 116.121 \pm 0.021$  ms with a reduced  $\chi^2$  value of 1.006. Combining the average  $^{62}\text{Ga}$  half-life with recent measurements of the  $^{62}\text{Ga}$  decay  $Q$  value and the superallowed  $\beta$ -branching ratio yields  $ft = 3074.3(12)$  s for  $^{62}\text{Ga}$ , which has been reduced by  $0.9\sigma$  from its previous value [7]. The  $^{62}\text{Ga}$   $ft$  value is now known to  $\pm 1.2$  s, or 0.04%, and rivals the precision of the best known superallowed  $ft$  values for  $A < 62$ . This high-precision superallowed  $ft$  value provides a new benchmark for tests of isospin symmetry breaking calculations for  $A \geq 62$  superallowed  $\beta$  decays. Improved precision in the theoretical radiative corrections for the the high- $Z$  superallowed emitters will,

however, be required to improve this test. The precision of the experimental  $^{62}\text{Ga}$   $ft$  value is now limited by the precision in the statistical rate function  $f$  that results from a single high-precision  $Q$ -value measurement [8] and an independent confirmation of this result would also be highly desirable.

#### ACKNOWLEDGMENTS

We thank the ISAC and TRILIS members T. Achtzehn, D. Albers, P. Bricault, M. Dombisky, J. Lassen, J. P. Lavoie, and M. R. Pearson for their hard work and dedication to the production of the high-quality  $^{62}\text{Ga}$  beams necessary for these experiments. This work was partially supported by the Natural Sciences and Engineering Research Council of Canada, the Government of Ontario through a Premier's Research Excellence Award, the National Research Council of Canada, and the Research Corporation through a Research Innovation Award. TRIUMF receives federal funding via a contribution agreement through the National Research Council of Canada.

- 
- [1] J. C. Hardy and I. S. Towner, Phys. Rev. C **71**, 055501 (2005).  
 [2] J. C. Hardy and I. S. Towner, Phys. Rev. Lett. **94**, 092502 (2005).  
 [3] J. C. Hardy, arXiv:hep-ph/0703165 (2007).  
 [4] W. J. Marciano and A. J. Sirlin, Phys. Rev. Lett. **96**, 032002 (2006).  
 [5] I. S. Towner, J. C. Hardy, and M. Harvey, Nucl. Phys. **A284**, 269 (1977); I. S. Towner and J. C. Hardy, Phys. Rev. C **66**, 035501 (2002).  
 [6] W. E. Ormand and B. A. Brown, Phys. Rev. C **52**, 2455 (1995); Phys. Rev. Lett. **62**, 866 (1989); Nucl. Phys. **A440**, 274 (1985).  
 [7] B. Hyland *et al.*, Phys. Rev. Lett. **97**, 102501 (2006).  
 [8] T. Eronen *et al.*, Phys. Lett. **B636**, 191 (2006).  
 [9] B. Blank *et al.*, Phys. Rev. C **69**, 015502 (2004).  
 [10] C. Geppart *et al.*, Nucl. Phys. **A746**, 631c (2004).  
 [11] V. T. Koslowsky, E. Hagberg, J. C. Hardy, R. E. Azuma, E. T. H. Clifford, H. C. Evans, H. Schmeing, U. J. Schrewe, and K. S. Sharma, Nucl. Phys. **A405**, 29 (1983).  
 [12] E. Hagberg *et al.*, Nucl. Phys. **A571**, 555 (1994).  
 [13] V. T. Koslowsky, E. Hagberg, J. C. Hardy, G. Savard, H. Schmeing, K. S. Sharma, and X. J. Sun, Nucl. Instrum. Methods A **401**, 289 (1997).  
 [14] G. F. Grinyer *et al.*, Phys. Rev. C **71**, 044309 (2005).  
 [15] A. P. Baerg, Metrologia **1**, No. 3, 131 (1965).  
 [16] W. H. Press *et al.*, *Numerical Recipes in C*, 2nd ed. (Cambridge University Press, New York, 1992).  
 [17] S. Baker and R. D. Cousins, Nucl. Instrum. Methods A **221**, 437 (1984).  
 [18] P. Finlay *et al.* (to be published, 2008).  
 [19] C. E. Svensson *et al.*, Nucl. Instrum. Methods B **204**, 660 (2003).  
 [20] G. C. Ball *et al.*, J. Phys. G **31**, S1491 (2005).  
 [21] P. E. Garrett *et al.*, Nucl. Instrum. Methods B **261**, 1084 (2007).  
 [22] B. E. Zimmerman, M. P. Unterwieser, and J. T. Cessna, J. Phys. G **23**, 1707 (1997).  
 [23] H. Junde and B. Singh, Nucl. Data Sheets **91**, 317 (2000).  
 [24] E. Runte *et al.*, Nucl. Phys. **A399**, 163 (1983).  
 [25] W.-M. Yao *et al.*, J. Phys. G **33**, 1 (2006).  
 [26] M. Hannawald *et al.*, Phys. Rev. Lett. **82**, 1391 (1999).  
 [27] D. E. Alburger, Phys. Rev. C **18**, 1875 (1978).  
 [28] C. N. Davids, C. A. Gagliardi, M. J. Murphy, and E. B. Norman, Phys. Rev. C **19**, 1463 (1979).  
 [29] B. C. Hyman *et al.*, Phys. Rev. C **68**, 015501 (2003).  
 [30] G. Cachel *et al.*, Eur. Phys. J. A **23**, 409 (2005).  
 [31] B. Hyland *et al.*, J. Phys. G **31**, S1885 (2005).  
 [32] J. C. Hardy (private communication, 2007).  
 [33] A. Czarnecki, W. J. Marciano, and A. Sirlin, Phys. Rev. D **70**, 093006 (2004).